Time-Resolved Fluorometric and Differential Scanning Calorimetric Investigation of Dehydroergosterol in 1-Stearoyl-2-caprylphosphatidylcholine Bilayers†

Yvonne Lin Kao,‡ Parkson Lee-Gau Chong,*,‡ and Ching-hsien Huang§

Department of Biochemistry, Meharry Medical College, Nashville, Tennessee 37208, and Department of Biochemistry, University of Virginia School of Medicine, Charlottesville, Virginia 22908

Received August 7, 1989; Revised Manuscript Received October 3, 1989

ABSTRACT: Thermal and dynamic properties of dehydroergosterol (DHE) in 1-stearoyl-2-capryl-*sn*-glycero-3-phosphocholine [C(18):C(10)PC] have been studied by differential scanning calorimetry (DSC) and multifrequency phase-modulation fluorometry. C(18):C(10)PC is an asymmetric mixed-chain phosphatidylcholine known to form highly ordered mixed interdigitated bilayers below the maximal transition temperature, T_m, and partially interdigitated bilayers above T_m. This lipid system is thus unique in assessing the interactions between sterols and interdigitated lipid bilayers. DHE is a fluorescent analogue of cholesterol shown in previous studies to behave like cholesterol in noninterdigitated symmetric diacylphosphatidylcholines. DSC data show that DHE exhibits similar characteristics to cholesterol [Chong & Choate (1989) *Biophys. J. 55*, 551–556] in C(18):C(10)PC bilayers. DHE abolishes the phase transition of C(18):C(10)PC at 27 mol % compared to 25 mol % for cholesterol and decreases T_m, the onset temperature (T_o), and the completion temperature (T_c), at a similar rate to cholesterol at about −0.25 °C per mole percent DHE. Fluorescence data show that the rotational motion of DHE can be described by a hindered anisotropic model. In the gel state of C(18):C(10)PC, the rotational correlation time of DHE decreases monotonically with increasing DHE content up to 24 mol %, suggesting that DHE causes a disordering/spacing effect on the packing of mixed interdigitated C(18):C(10)PC bilayers. The rotational correlation time undergoes an abrupt increase from 24 to 27 mol % DHE. Abrupt changes in the DSC parameters were also observed in the neighborhood of 27 mol %, suggesting that major reorganization takes place around this concentration. The rotational data support the idea (Chong & Choate, 1989) that sterols may have a function in preventing lipids from forming highly ordered interdigitated structures in natural membranes.

The existence of highly ordered interdigitated lipid bilayers in synthetic phospholipid vesicles has been shown through a variety of physical and chemical situations [reviewed in Huang and Mason (1986) and Slater and Huang (1988)]; however, whether lipid interdigitation exists in cellular membranes, though believed, for example, in sphingomyelins (Levin et al., 1985), has not yet been proven for technical reasons. The presence of interdigitated bilayers which can result from asymmetric mixed-chain phospholipids would provide an adverse environment for cellular membranes, since optimal membrane functions usually require appropriate lipid fluidity (Singer & Nicolson, 1972). To investigate the possible existence of interdigitation in biological systems, further characterization of model systems can be used. Initial studies of interdigitation have mainly focused on single-component systems, but in order to mimic real-life, studies should be extended to include other membrane constituents; one, in particular, is cholesterol which can comprise a large amount of a cell and has been shown to have a great influence on membrane properties by altering fluidity.

In this study, 1-stearoyl-2-capryl-*sn*-glycero-3-phosphocholine [C(18):C(10)PC][1] was employed as the model interdigitated lipid. C(18):C(10)PC contains an *sn*-1 acyl chain which is twice the length of the *sn*-2 acyl chain. This type of asymmetric mixed-chain phosphatidylcholine is known to form highly ordered mixed interdigitated bilayers below the transition temperature, T_m, and relatively disordered partially interdigitated bilayers above the transition as shown through extensive studies (Mason et al., 1981; Huang et al., 1982, 1983; McIntosh et al., 1984; Hui et al., 1984; Xu & Huang, 1987; Mattai et al., 1987; Wong & Huang, 1989). The interactions of C(18):C(10)PC with fatty acid spin-labels (Boggs & Mason, 1986) and with symmetric diacylphosphatidylcholine (Mason, 1988) have also been reported.

Recently, Chong and Choate (1989) using differential scanning calorimetry (DSC) studied the thermal behavior of binary mixtures comprised of C(18):C(10)PC and cholesterol. It was reported that incorporation of a low level (~25 mol %) of cholesterol is sufficient to abolish the phase transition of C(18):C(10)PC. As a comparison, a high level of cholesterol is needed to abolish the phase transition of noninterdigitated phosphatidylcholines of similar hydrocarbon chain

† This work was supported in part by a grant from the National Science Foundation (NSF-MRCE, Grant R11-8714805 to Meharry Medical College), by a grant from the U.S. Army Research Office (to P.L.-G.C.), and in part by a grant from the National Institutes of Health (GM 17452 to C.H.). This work was done during the tenure of an Established Investigatorship (to P.L.-G.C.) from the American Heart Association and CIBA GEIGY. Y.L.K. is a recipient of the Patricia-Roberts-Harris Fellowship. The experiments and analyses of the fluorescence data were performed at the Laboratory for Fluorescence Dynamics (LFD) at the University of Illinois at Urbana—Champaign (UIUC). The LFD is supported jointly by the Division of Research Resources of the National Institutes of Health (RR03155-01) and UIUC.

* Address correspondence to this author.
‡ Meharry Medical College.
§ University of Virginia School of Medicine.

[1] Abbreviations: C(18):C(10)PC, 1-stearoyl-2-capryl-*sn*-glycero-3-phosphocholine; DHE, dehydroergosterol [$\Delta^{5,7,9(11),22}$-ergostatetraen-3β-ol]; DMPC, dimyristoylphosphatidylcholine; DPPC, dipalmitoylphosphatidylcholine; DSC, differential scanning calorimetry; POPOP, 1,4-bis(5-phenyl-2-oxazolyl)benzene; POPC, 1-palmitoyl-2-oleoyl-L-α-phosphatidylcholine; DLPE, dilauroylphosphatidylethanolamine.

0006-2960/90/0429-1315$02.50/0

length (Ladbrooke et al., 1968; Hinz & Sturtevant, 1972; Estep et al., 1978). It was also found that cholesterol lowers both the enthalpy changes of the phase transition, ΔH, and the transition temperature, T_m (Chong & Choate, 1989). Also, the decreasing rate of T_m in cholesterol/C(18):C(10)PC is greater than that for cholesterol in DMPC, a noninterdigitated lipid bilayer under normal conditions. The high cholesterol sensitivity to the phase transition between interdigitated lipid bilayers was attributed to the fact that the formation of highly ordered interdigitated lipid bilayers requires stringent structural conditions such as specific chain length differences and high molecular order. It was believed that in the presence of cholesterol, these stringent structural conditions are no longer satisfied as the result of a disordering effect of cholesterol on mixed interdigitated bilayers. However, calorimetric data provide very limited structural information. It is not yet clear how cholesterol disrupts the packing of C(18):C(10)PC.

The purpose of the present study is to use a fluorescent cholesterol analogue to provide more information about how sterols affect the packing of interdigitated C(18):C(10)PC bilayers. This goal is achieved by using binary mixtures comprising of C(18):C(10)PC and dehydroergosterol [$\Delta^{5,7,9(11),22}$-ergostatetraen-3β-ol; abbreviated as DHE). DHE is a naturally occurring fluorescent cholesterol analogue with physical and physiological properties resembling cholesterol (Archer, 1975; Rogers et al., 1979; Hale & Schroeder, 1982; Yeagle et al., 1982; Schroeder et al., 1987; Nemecz et al., 1988; Bar et al., 1989; Chong et al., 1989). In this study, DSC was employed to ensure that DHE in C(18):C(10)PC exhibits phase behavior similar to cholesterol in C(18):C(10)PC (Chong & Choate, 1989). Then, multifrequency phase-modulation fluorometry was employed to obtain fluorescence anisotropy decay data of DHE in C(18):C(10)PC as a function of DHE content at two temperatures. The anisotropy decay data allow the rotational correlation time and the limiting anisotropy to be determined. These parameters have provided more direct evidence for the sterol-induced disordering/spacing effects on mixed interdigitated C(18):C(10)PC. A preliminary report of this work has appeared elsewhere (Kao & Chong, 1989).

Materials and Methods

Materials. DHE was obtained from Frann Scientific Inc. (Columbia, MO) and was purified by high-performance liquid chromatography according to Chong and Thompson (1986). C(18):C(10)PC was synthesized by the method of Xu and Huang (1987). DMPC and DPPC were purchased from Avanti Polar Lipids (Birmingham, AL). Cholesterol was purchased from Nu-Chek Prep. Inc. (Elysian, MN). 1,4-Bis(5-phenyl-2-oxazolyl)benzene (POPOP) was purchased from Eastman Kodak Co. (Rochester, NY). Acrylamide purchased from Bio-Rad (Rockville Center, NY) was recrystallized from ethyl acetate. DHE concentration was determined by using an extinction coefficient at 326 nm, in dioxane equal to 10 600 $M^{-1}\cdot cm^{-1}$ (Muczynski & Stahl, 1983).

Preparation of Liposomes. DHE dissolved in dioxane and phospholipids dissolved in chloroform were mixed in proportions as indicated in the legends to the figures and tables. The mixtures were dried under vacuum overnight and then suspended in 50 mM KCl. The samples were heated to 37 °C [pure C(18):C(10)PC T_m is 19.3 °C] for 20 min under nitrogen and then vortexed for 5 min at 37 °C. The samples were then placed at 0 °C for 20–60 min to anneal. The freeze–thaw cycle was repeated 2 more times before the samples were stored at 4 °C for 48 h. Phospholipid concentrations were determined by the method of Bartlett (1959).

A long-term low-temperature sample was stored for 29 days at −20 °C to determine if sample history is a factor affecting phase transition in interdigitated lipids.

Calorimetric Measurements. Calorimetric measurements were made with a Hart Scientific differential scanning calorimeter (Provo, UT) which contains four ampules: three for samples and one as a reference. The samples were loaded above room temperature to prevent condensation forming in the calorimeter. The temperature was immediately brought down to 0 °C and held for 15 min before the heating scan was initiated. The sample was heated to 45 °C and then held for 15 min before a cooling scan was conducted down to 0 °C. The samples were subjected to two heating and cooling scans. Both the heating and cooling scans were made at a scan rate of 15 °C/h. At this slow scan rate, the thermogram does not need to be corrected for instrument response.

DPPC was used to calibrate the DSC in the event of machine hysteresis since DPPC is known to exhibit an identical T_m for the main phase transition on both heating and cooling (Lentz et al., 1978). Dried DPPC was suspended in 50 mM KCl and vortexed at 50–60 °C to form multilamellar vesicles; 1 mM DPPC solution was loaded into each sample ampule. The DPPC samples were scanned from 15 to 60 °C through two heating and cooling cycles. The differences between the heating onset temperature and cooling onset temperature are the machine hysteresis. DPPC results show that machine hysteresis is dependent upon the ampule in which the sample is loaded. The machine hystereses for the first, second, and third sample ampules were 0.923, 0.974, and 0.872 °C, respectively. The cooling temperatures were corrected with their respective values to give the true thermal hysteresis between the heating and cooling scans.

Fluorescence Measurements. Fluorescence lifetimes and anisotropy decays of dehydroergosterol in C(18):C(10)PC bilayers were determined at the Laboratory for Fluorescence Dynamics at the University of Illinois at Urbana—Champaign using a multifrequency phase and modulation fluorometer (Gratton & Limkeman, 1983). The light source was a He/Cd laser (Model 4240B, Liconix Inc., Sunnyvale, CA). The excitation wavelength used was 325 nm. The light was modulated by the use of two standing-wave acousto-optic modulators (Piston et al., 1989). For lifetime measurements, the excitation polarizer was set at 35° with respect to the vertical plane, and no emission polarizer was used. Phase and modulation values were determined relative to a POPOP (in ethanol) reference solution, which has a lifetime of 1.35 ns at 325-nm excitation. For anisotropy decay measurements, differential phase and demodulation ratio between parallel and perpendicular components were determined, upon vertical excitation (Weber, 1978; Lakowicz et al., 1984). A Schott KV-389 cutoff filter was used for DHE emission for both the intensity decay and the anisotropy decay measurements. Phase (or differential phase) and modulation (or demodulation ratio) were determined with the modulation frequencies ranging from 20 to 160 MHz. The data were analyzed by using the nonlinear least-squares program provided by the Laboratory for Fluorescence Dynamics based on the scheme described elsewhere (Jameson & Gratton, 1983; Lakowicz et al., 1984, 1985). Random errors of 0.2° for the phase angle and 0.004 for modulation values were used in the least-squares fit. The goodness of the fit is judged by the reduced χ^2. The samples that were measured at 3.9 °C were not exposed to temperatures above the T_m. To obtain comparable DSC and fluorescence data, each sample was measured at 3.9 °C first, and incubated at about 4 °C before measurement at 31.4 °C.

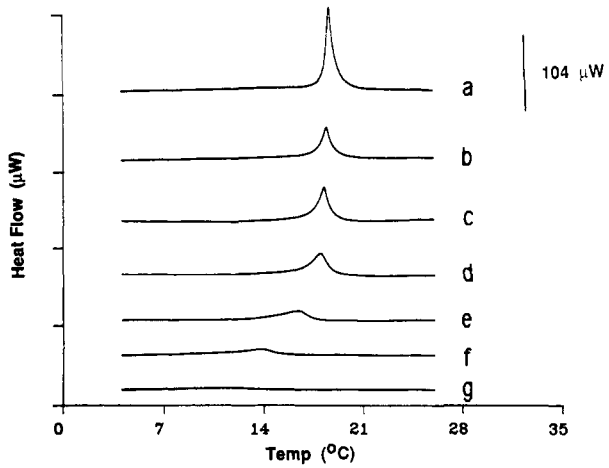

FIGURE 1: Typical heating DSC curves of C(18):C(10)PC in the presence of DHE. Listed in the figure are the molar ratios of DHE in the mixture. The phospholipid concentrations of the measured samples are (a) 1.11 mM for pure C(18):C(10)PC, (b) 0.96 mM for 1.10 mol %, (c) 1.26 mM for 2.02 mol %, (d) 0.95 mM for 3.03 mol %, (e) 0.92 mM for 9.41 mol %, (f) 1.01 mM for 22.06 mol %, and (g) 1.40 mM for 27.09 mol %. 400 μL of the lipid dispersions was used for each sample measurement.

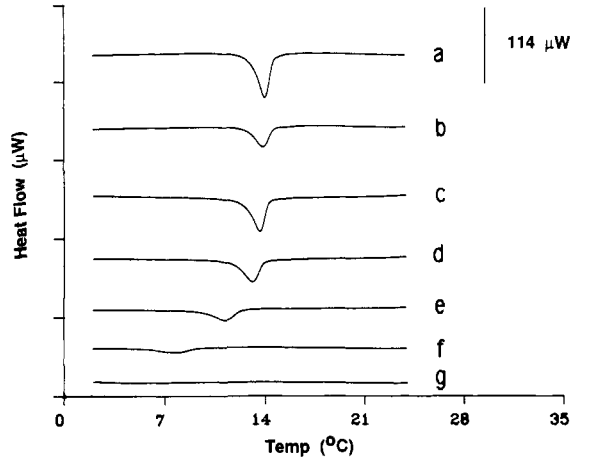

FIGURE 2: Cooling DSC curves of DHE in C(18):C(10)PC. The phospholipid concentrations of the measured samples (a–f) are listed in Figure 1.

The acrylamide quenching experiment was performed using a Greg 200 fluorometer (ISS Inc., Champaign, IL).

RESULTS

DSC Measurements. The heating DSC curves in Figure 1 show the effect of increasing DHE content on the phase behavior of binary mixture of DHE/C(18):C(10)PC dispersed in 50 mM KCl. The sharp endothermic transition peak of pure C(18):C(10)PC at 18.8 °C is progressively broadened as the DHE amount is increased; this broadening is accompanied by a slight shift in T_m to lower temperatures. The transition peak is abolished completely at about 27 mol % DHE. Figure 2 shows cooling DSC curves of DHE/C(18):C(10)PC mixtures with increasing mole fraction of DHE up to 27 mol %. As with the heating data, the endothermic transition peak is also abolished at 27 mol % DHE. Figure 3a shows a decrease in the total enthalpy change, ΔH, as the DHE content is increased. At 27 mol % DHE, the totally enthalpy change is virtually zero. An increase in DHE content results in a decrease in apparent transition entropy (Figure 3b). Panels a and b of Figure 4 show the effect of increasing DHE content on the onset temperature, T_o, the maximum temperature, T_m, and the completion temperature, T_c, for heating and cooling

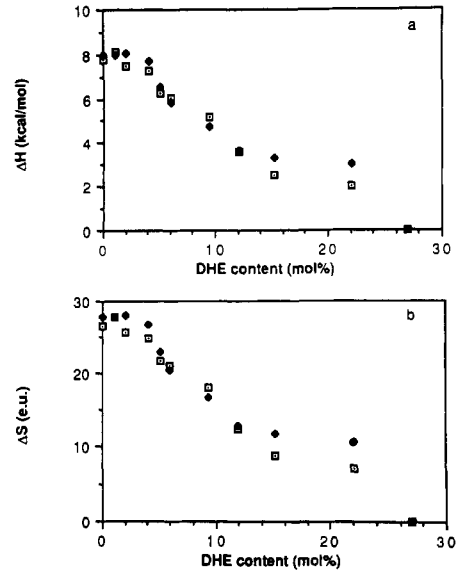

FIGURE 3: (a) Effect of increasing DHE content on the total enthalpy change of C(18):C(10)PC. (b) DHE dependence of the apparent entropy change, ΔS, calculated by $\Delta S = \Delta H/T_m$. "e.u" stands for "entropy unit". (♦) Cooling; (⊡) heating.

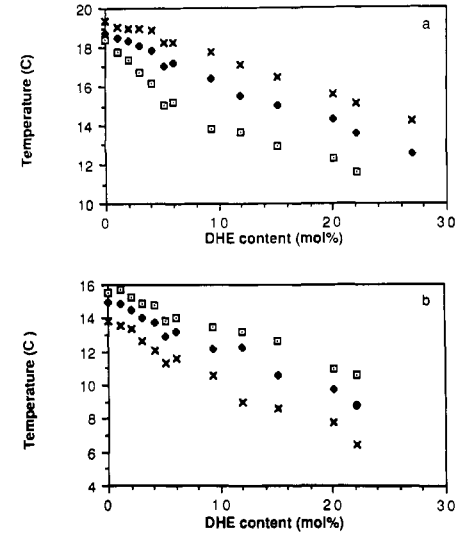

FIGURE 4: (a) DHE heating dependence of T_m, T_o, and T_c in C(18):C(10)PC. (b) DHE cooling dependence of T_m, T_o, and T_c in C(18):C(10)PC. (⊡) T_o; (♦) T_m; (×) T_c.

scans, respectively. T_o and T_c were determined by the method shown in Figure 2 of Xu et al. (1987). These values were corrected for machine hysteresis. In both ascending and descending temperature scans, T_m, T_o, and T_c decrease with increasing DHE. The decreasing rates are estimated to be −0.29 °C/mol % sterol for T_o, −0.23 °C/mol % for T_m, and −0.19 °C/mol % for T_c. The cooling rates are −0.32 °C/mol % for T_c, −0.27 °C/mol % for T_m, and −0.23 °C/mol % for T_o.

A partial phase diagram of DHE/C(18):C(10)PC binary mixtures was constructed by using the T_o of the heating and cooling scans. The phase diagram (not shown) is similar to that obtained for cholesterol in C(18):C(10)PC (Chong & Choate, 1989).

A 12 mol % DHE/C(18):C(10)PC sample which was incubated for 29 days at −20 °C exhibited no new transition peak. The thermodynamic parameters derived from this sample were almost identical with those derived from other samples (data not shown). Thus long-term incubation at low temperatures of DHE/C(18):C(10)PC mixtures results in no

Table I: Analysis of Fluorescence Emission Decay of Dehydroergosterol in C(18):C(10)PC[a]

temp (°C)	mol % DHE	τ_1 (ns)	f_1	α_1	τ_2 (ns)	χ^2	$\langle\tau\rangle$ (ns)
3.9	1	1.40 ± 0.05	0.86	0.93	3.16 ± 0.75	1.69	1.65
	2	1.43 ± 0.06	0.88	0.95	3.55 ± 1.09	1.59	1.69
	5	1.33 ± 0.02	0.93	0.98	5.27 ± 0.91	0.55	1.62
	9	1.04 ± 0.09	0.63	0.80	2.40 ± 0.32	2.37	1.54
	15	1.14 ± 0.04	0.72	0.86	2.74 ± 0.21	0.59	1.58
	24	1.22 ± 0.06	0.82	0.92	3.18 ± 0.74	1.69	1.57
	27	1.06 ± 0.43	0.75	0.89	2.84 ± 0.29	1.52	1.52
	35	0.81 ± 0.08	0.45	0.67	1.99 ± 0.14	1.96	1.46
31.4	2	0.66 ± 0.05	0.87	0.95	1.70 ± 0.52	0.39	0.80
	5	0.70 ± 0.01	0.96	0.99	3.68 ± 1.08	1.06	0.81
	20	0.58 ± 0.06	0.60	0.76	1.23 ± 0.12	0.28	0.84
	24	0.69 ± 0.02	0.91	0.98	2.73 ± 0.58	1.28	0.82
	27	0.73 ± 0.01	0.90	0.97	2.43 ± 0.32	0.76	0.90
	35	0.77 ± 0.01	0.92	0.98	3.25 ± 0.42	0.93	0.97

[a] $f_2 = 1 - f_1$ and $\alpha_2 = 1 - \alpha_1$.

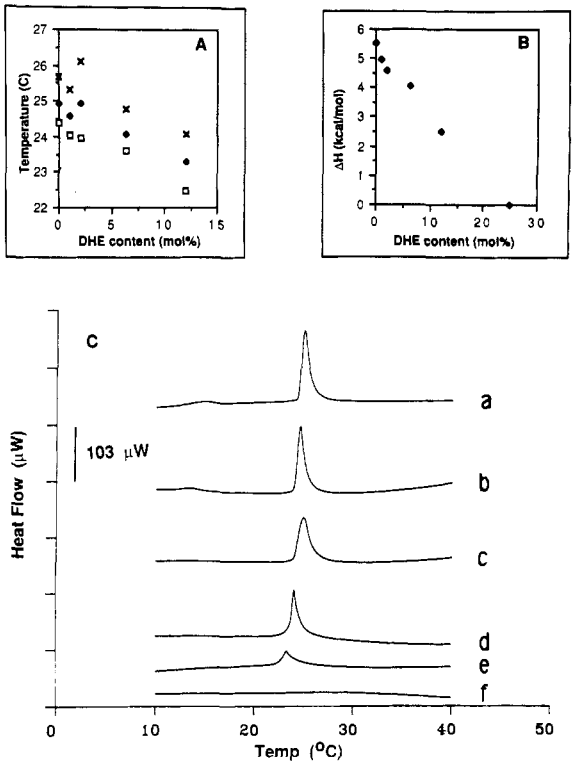

FIGURE 5: (A) DHE heating dependence of T_m (♦), T_o (⊡), and T_c (×) in DMPC multilamellar vesicles. (B) Effect of increasing DHE content on the total enthalpy change of DMPC multilamellar vesicles. (C) Typical heating DSC curves of DMPC in the presence of DHE. The phospholipid concentrations of the measured samples are (a) 1.11 mM for pure DMPC, (b) 3.68 mM for 1.00 mol %, (c) 4.13 mM for 2.10 mol %, (d) 6.30 mM for 6.30 mol %, (e) 3.77 mM for 13.01 mol %, and (f) 3.24 mM for 25.00 mol %. 400 μL of the lipid disperions was used for each sample measurement.

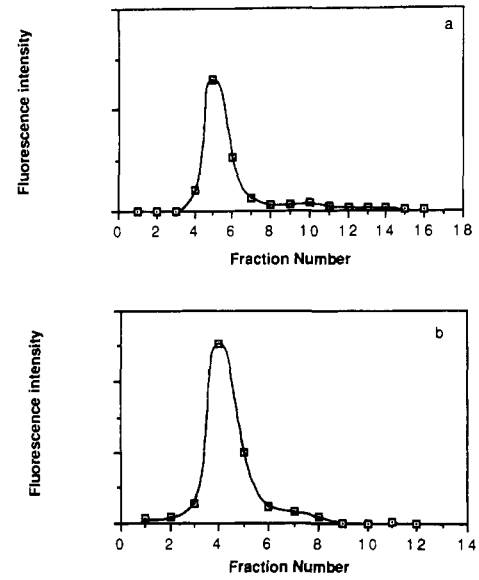

FIGURE 6: Elution profile of 12 mol % DHE in C(18):C(10)PC on a Sepharose CL-2B column (1 × 3.2 cm) at (a) 24 °C and (b) 4 °C. The column was eluted with 50 mM KCl. 200-μL fractions were collected and aliquots measured for fluorescence intensity at λ_{ex} = 325 nm.

new phase, unlike pure C(18):C(10)PC (Boggs & Mason, 1986).

In order to compare the thermal behavior of DHE/C(18):C(10)PC with that in noninterdigitated lipid bilayers, a series of DSC scans for DHE in dimyristoylphosphatidylcholine (DMPC) were carried out (Figure 5C). Unlike DHE in C(18):C(10)PC, a pretransition peak is observed in DHE/DMPC at about 15 °C. This pretransition peak is abolished by 3 mol % DHE. It is noticed that the main phase transition peak for DHE/DMPC is slightly asymmetric whereas that of DHE/C(18):C(10)PC is relatively more symmetric. Both systems show a decrease in T_m with increase in DHE content, but with significantly different rates: −0.15 °C/mol % sterol for DHE/DMPC (Figure 5A) and −0.23 to −0.27 °C/mol % sterol for DHE/C(18):C(10)PC. The phase transition of DMPC is abolished at about 25 mol % DHE (Figure 5B). Note that Hale and Schroeder (1982) reported that 42 mol % DHE is needed to abolish the phase transition of DPPC.

Column Chromatography. The elution profiles of 12 mol % DHE in C(18):C(10)PC after a Sepharose 2B column carried out below the T_m (4 °C) and above the T_m (27 °C) are shown in panels a and b, respectively, of Figure 6. Note that the transition temperature range of 12 mol % DHE in C(18):C(10)PC is about 8–18 °C (Figure 4). The y axis is the fluorescence intensity of DHE. A single sharp peak is observed at both temperatures, demonstrating that the vesicle size remains almost unchanged both above and below the transition temperature and that no DHE micelles are noticeable.

Fluorescence Lifetime. The measured phase delay and modulation data were fitted to the exponential decay law:

$$I(t) = \sum \alpha_i \exp(-t/\tau_i)$$

where $I(t)$ is the fluorescence intensity, α_i is the preexponential factor, and τ_i is the fluorescence lifetime from the ith component. Table I shows the best fitted decay parameters as a function of DHE content in C(18):C(10)PC at 3.9 °C ($<T_m$) and at 31.4 °C ($>T_m$). Note in Table I that $f_i = \alpha_i\tau_i/\sum\alpha_j\tau_j$

Table II: Analysis of Fluorescence Anisotropy Decay of Dehydroergosterol in C(18):C(10)PC[a]

temp (°C)	mol % DHE	$r_1 = r_\infty$	θ_2 (ns)	r_2	χ^2
3.9	1	0.07 ± 0.02	1.81 ± 0.89	0.08 ± 0.01	3.39
	2	0.06 ± 0.01	1.66 ± 0.38	0.07 ± 0.00	0.55
	5	0.08 ± 0.01	1.14 ± 0.70	0.08 ± 0.01	2.64
	9	0.10 ± 0.01	0.68 ± 0.39	0.08 ± 0.01	1.66
	20	0.10 ± 0.00	0.41 ± 0.20	0.10 ± 0.02	1.18
	24	0.13 ± 0.01	0.20 ± 0.26	0.19 ± 0.17	1.87
	27	0.11 ± 0.01	0.86 ± 0.27	0.09 ± 0.00	0.99
	35	0.11 ± 0.00	0.68 ± 0.21	0.09 ± 0.01	0.82
31.4	2	0.13 ± 0.01	0.39 ± 0.15	0.18 ± 0.02	0.65
	20	0.09 ± 0.01	0.81 ± 0.25	0.14 ± 0.00	0.76
	24	0.09 ± 0.01	1.00 ± 0.24	0.15 ± 0.01	0.32
	27	0.10 ± 0.01	0.48 ± 0.24	0.15 ± 0.02	1.36
	35	0.08 ± 0.01	0.71 ± 0.27	0.13 ± 0.00	1.08

[a] θ_1 is fixed to 10 000 ns.

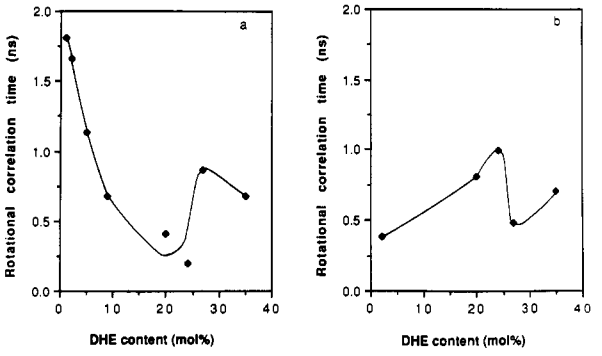

FIGURE 7: Effect of increasing DHE content on the rotational correlation time θ_2 at (a) 3.9 °C and (b) 31.4 °C of DHE in C(18):C(10)PC vesicles. λ_{ex} = 325 nm. The uncertainties of the data have been shown in Table II.

where f_i is the fraction of the total fluorescence intensity derived from the ith component. DHE emission in C(18):C(10)PC is best described by a double-exponential decay over the entire concentration range examined.

The average lifetime, $\langle\tau\rangle = (\tau_1)f_1 + (\tau_2)f_2$, is also listed in Table I. The $\langle\tau\rangle$ increases with increasing DHE content at 31.4 °C but decreases with DHE content at 3.9 °C. In contrast, Schroeder et al. (1987) reported τ is almost invariant with DHE content in the fluid state of 1-palmitoyl-2-oleoylphosphatidylcholine (POPC).

Anisotropy Decay Measurement. The data of differential phase and demodulation ratio are fitted by the equation $(r(t) = r_1e^{-t/\theta_1} + r_2e^{-t/\theta_2}$. In fitting the data, we fixed θ_1 = 10 000 ns and let r_1 become the floating parameter. In this case, r_1 is essentially the limiting anisotropy r_∞. It is judged from the reduced χ^2 that, among other models tested, the equation $r(t) = r_\infty + r_2e^{-t/\theta_2}$ best fits the data. Table II lists the fitted limiting anisotropy and rotational correlation times, θ_2, for increasing DHE concentration in C(18):C(10)PC. Table II shows that the r_∞ at 3.9 °C remains relatively constant near 0.1 despite the increase in DHE. Figure 7a demonstrates the values from Table II for the effect of DHE content on θ_2 at 3.9 °C. The θ_2 decreases monotonically from 1.8 ns at 1 mol % to 0.2 ns at 24 mol %, where at 27 mol % the θ_2 increases to 0.8 ns and decreases again above 27 mol %.

Table II also shows the effect of DHE above the phase transition of C(18):C(10)PC on the r_∞. Again, r_∞ was found to be around 0.1. Figure 7b exhibits a steady increase in θ_2, as DHE content is increased from 0.39 ns at 2 mol % DHE until 0.99 ns for 24 mol % DHE. At 27 mol %, the θ_2 abruptly decreases to 0.47 ns. After 27 mol % DHE, θ_2 steadily increases.

Table III: Quenching Rate Constant, k^*, as a Function of DHE Content at 3.9 °C[a]

mol % DHE	K_{sv} (M^{-1})	τ_0 (ns)	k^* (ns^{-1} M^{-1})
1	0.22	1.65	0.13
2	0.27	1.69	0.16
5	0.23	1.62	0.14
9	0.23	1.54	0.15
20	0.22	1.41	0.16

[a] The fluorescence intensities at 375 nm were recorded and corrected for background signals and for volume changes. λ_{ex} = 325 nm.

Acrylamide Quenching. The fluorescence intensity quenching of DHE in C(18):C(10)PC by acrylamide at 3.9 °C give a linear Stern–Volmer plot at [acrylamide] <2 M for all the DHE/C(18):C(10)PC samples examined (data not shown). Using the average lifetime listed in Table I and assuming a dynamic quenching mechanism, we can calculate the quenching rate constant, k^*, by using the equation $F^0/F = 1 + k^*\tau_0$[acrylamide]. The resulting k^* values are listed in Table III. k^* is almost invariant (0.13–0.16 ns^{-1} M^{-1}) with DHE content, indicating that the accessibility of DHE to acrylamide does not change significantly as the DHE content varies.

Discussion

The DSC results show similar effects of DHE vs cholesterol on the phase behavior of C(18):C(10)PC. The phase transition of C(18):C(10)PC can be abolished by about 27 mol % DHE (Figures 1 and 3); similarly, incorporation of about 25 mol % cholesterol eliminates the phase transition in the calorimetric scan of C(18):C(10)PC/cholesterol mixtures (Chong & Choate, 1989). Furthermore, the rates for the decrease in T_m, T_o, and T_c [Figure 4 in this paper and in Chong and Choate (1989)] in both systems (DHE vs cholesterol) are also similar (about −0.25 °C/mol % sterol). This is additional evidence showing that DHE resembles cholesterol in their physical and physiological properties as previously described in the introduction. Moreover, the decreasing rates of T_m, T_o, and T_c with increasing DHE content in C(18):C(10)PC are significantly different from those of DHE in DMPC (Figure 5): −0.15 °C/mol % DHE for DHE in DMPC and about −0.25 °C/mol % DHE for DHE in C(18):C(10)PC. From this point of view, the phase transition of interdigitated lipids [e.g., C(18):C(10)PC] is more sensitive to DHE than the phase transition of noninterdigitated lipids (e.g., DMPC). A similar conclusion has been obtained in the case of cholesterol in C(18):C(10)PC (Chong & Choate, 1989).

On the basis of calorimetric data on C(18):C(10)PC/cholesterol mixtures, Chong and Choate (1989) proposed that cholesterol molecules insert into the mixed interdigitated structure of C(18):C(10)PC and disrupt the coupling between the opposing leaflets in the highly ordered bilayer of C(18):C(10)PC at $T < T_m$. In the present study, phase modulation fluorometry was employed to verify earlier results on similar C(18):C(10)PC/DHE mixtures. The differential phase and demodulation method allows the rotational correlation time and the limiting anisotropy to be determined. These parameters reflect the volume available for DHE rotation and the hindrance experienced by DHE.

The rotational correlation time θ_2 of DHE in C(18):C(10)PC at 3.9 °C decreases monotonically with increasing DHE content up to 24 mol % DHE (Figure 7a). Since the rotational correlation time is inversely proportional to the rotational rate, it can be concluded from Figure 7a that the rotation of DHE becomes faster as the content of DHE is increased up to 24 mol % due to the disordering/spacing effect

by DHE on the packing of originally highly ordered mixed interdigitated bilayers. This conclusion is in good agreement with that previously suggested by the DSC results in the case of cholesterol in C(18):C(10)PC (Chong & Choate, 1989). The agreement suggests that this effect of disordering is not specific for cholesterol; any bulky, rigid, cholesterol-like molecules may disrupt the highly ordered mixed interdigitated bilayers to a similar extent. Although previous Raman spectroscopic studies (Huang et al., 1982, 1983) show that the hydrocarbon chains of pure C(18):C(10)PC in bilayers are highly ordered, even more ordered than the acyl chains of DMPC in the gel state, the data shown in Figure 7a and Table II indicate considerable rotation for DHE in the gel state of C(18):C(10)PC/DHE mixtures (Figure 7a). For example, 1 mol % DHE in the gel state of C(18):C(10)PC shows a rotational correlation time of 1.8 ns (Figure 7a and Table II), whereas 0.9 mol % DHE in the gel state of DMPC has a comparable value of 1.4 ns (Smutzer, 1988b). This result echoes a recent study by Wong and Huang (1989), who used Fourier-transform infrared spectroscopy to show that the zigzag planes of the acyl chain of pure C(18):C(10)PC at temperature $< T_m$ have appreciable motions at atmospheric pressure and that only raising pressure higher than 5.5 kbar will completely damp the motion of the acyl chain. The results shown in the present study also suggest that at 1 atm, there is empty space around DHE for its rotation even in highly ordered interdigitated bilayers. It should be mentioned that it is not known yet whether C(18):C(10)PC maintains a highly ordered mixed interdigitated lipid bilayer in the presence of DHE. However, this is probably true for the cases at low DHE concentrations (e.g., 1 mol %) since the calorimetric parameters (Figures 1–4) show little differences between pure C(18):C(10)PC and C(18):C(10)PC containing 1 mol % DHE.

Since pure C(18):C(10)PC is in a disordered (Wong & Huang, 1989) partially interdigitated state at 31.4 °C, the increase in θ_2 with increasing DHE content between 2 and 24 mol % at 31.4 °C (Figure 7b) reflects an ordering effect on membranes by DHE. In summary, DHE has a dual function on C(18):C(10)PC: an ordering effect on lipid hydrocarbon chains at temperature $> T_m$ and a disordering/spacing effect at temperature $< T_m$. This situation is similar to cholesterol in symmetric diacylphosphatidylcholines (Cortijo et al., 1982).

A more detailed description of the rotation of DHE requires the knowledge of the direction of the emission dipole moment. Smutzer et al. (1986) mentioned that the emission transition dipole is likely to lie nearly colinear with the long axis of the sterol. If the long axis of the sterol is the cylindrical symmetry axis (Chong et al., 1985), the limiting anisotropy of DHE in highly ordered mixed interdigitated C(18):C(10)PC would have a high value approaching the fundamental anisotropy r_0 [r_0 = 0.36 (Smutzer et al., 1986), or 0.385 (Fischer et al., 1985), or 0.37 at 325-nm excitation (Chong & Thompson, 1986)]. Surprisingly, the limiting anisotropy values obtained in this study are much lower than the r_0 values. In fact, all the obtained limiting anisotropy values are below 0.13 (Table II). It should be pointed out that when the emission dipole moment is perpendicular to the cylindrical symmetry axis of the chromophore and the cylindrical symmetry axis is perpendicular to the lipid bilayer normal, as is the case for perylene, the limiting anisotropy should be low (Zannoni et al., 1983; Chong et al., 1985). It is likely that DHE resembles the situation of perylene, in which the emission transition dipole is perpendicular to the cylindrical symmetry axis of the chromophore which is nearly perpendicular to the bilayer normal. In this case, r_∞ should equal $0.1S^2$ where S is the order parameter. The finding that r_∞ is below 0.13 (Table II) may indicate that the order is essentially complete, and in this situation, the rotational rate should be more informative (Chong et al., 1985). If this is true, two rotations for DHE should be observed: the in-plane and out-of-plane rotations. The differential phase and demodulation ratio data are best fitted by the equation $r(t) = r_\infty + r_2 e^{-t/\theta_2}$, suggesting that only one of the dominating rotations is recovered in our measurements. (Note that r_0 is greater than $r_2 + r_\infty$.) Since the out-of-plane rotation is usually slower, the observed rotational correlation time, θ_2, should correspond to the out-of-plane rotation. The fast in-plane motion may be recovered by extending the modulation frequency beyond 160 MHz. The out-of-plane motion requires free volumes around the fluorophore; thus, the rotational correlation time θ_2 shown in Table II and Figure 7 should reflect the changes in volume experienced by DHE. Thus, the data shown in Figure 7a can be taken to indicate a disordering/spacing effect with increasing DHE content.

The presence of two DHE lifetime components (Table I) in lipid bilayers may represent two different environments as suggested by Nemecz and Schroeder (1988), who pointed out that the lifetime of the shorter component (the major component) increases as the environmental polarity increases. Our data in Table I show that at 3.9 °C the lifetime of the shorter component decreases with increasing DHE content, thus implying that the polarity around DHE decreases as DHE content increases (Nemecz & Schroeder, 1988). The changes in the polarity around DHE may be due to the changes in the vertical position of chromophore (the ring structure of DHE) with respect to the surface of C(18):C(10)PC. For example, sterol may be partially exposed in the aqueous medium at low concentrations and insert more deeper into the bilayer at high concentrations due to the disordering effect by sterols. However, the quenching data (Table III) argue against this possibility since the accessibility of DHE to acrylamide, in terms of the quenching rate constant k^*, seems to remain constant in the concentration region of 1–20 mol % DHE. An alternative explanation to the lifetime changes with DHE content is that DHE can form DHE-enriched domains in C(18):C(10)PC. The number and the size of the DHE-enriched domain may increase with increasing DHE content. The immediate environment around DHE must be different in different domains. Note that the formation of DHE-enriched domains in phospholipid bilayers has been previously suggested (Smutzer & Yeagle, 1985; Chong & Thompson, 1986).

Both the DSC and fluorescence data clearly show that something happened at about 27 mol % DHE. The DSC peak is abolished at about 27 mol %. The rotational correlation time derived from fluorescence studies has an abrupt change between 24 and 27 mol %. The peculiar phenomena at about 27 mol % may be attributed to the reorganization of DHE in C(18):C(10)PC, in a manner similar to the interpretation on the changes in physical parameters near 20–30 mol % in noninterdigitated lipid membranes. Formation of cholesterol-rich areas, cholesterol–cholesterol dimers, or cholesterol–phospholipid complexes was previously suggested to explain peculiar changes in physical parameters near 20–30 mol % sterol [reviewed in Houslay and Stanley (1982) and Hui (1988) and references cited therein]. Schroeder et al. (1987) noted that the limiting anisotropy and the rotational rate of DHE in the fluid state of POPC small unilamellar vesicles undergo abrupt changes near 33 mol % DHE. POPC under normal conditions is a noninterdigitated lipid. The

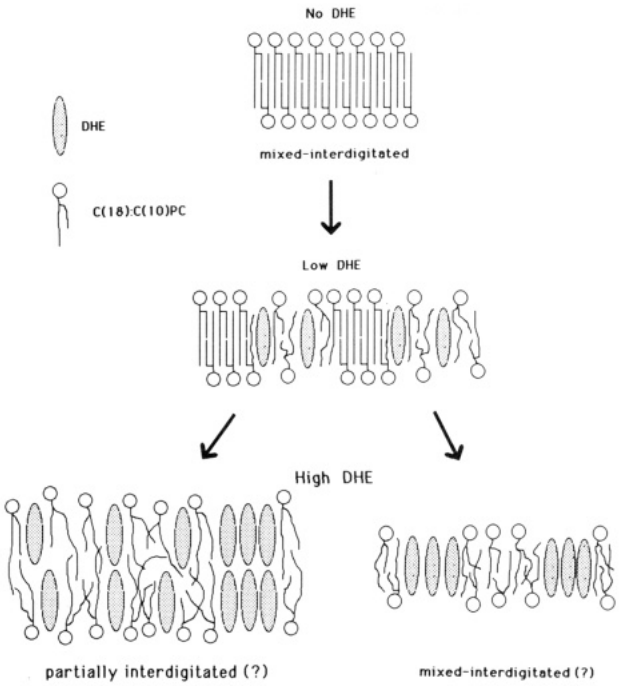

FIGURE 8: Model illustrating the disordering/spacing effect of increasing amounts of DHE in mixed interdigitated C(18):C(10)PC bilayers. The wavy lines represent disordered acyl chains.

peculiar phenomena at about 27 mol % DHE in C(18):C(10)PC cannot be attributed to fluorescence self-quenching since the peculiar behavior was also observed in DSC curves which are not governed by fluorescence properties.

On the basis of the data presented in this paper, the interaction of DHE with mixed interdigitated C(18):C(10)PC lipids can be depicted in Figure 8. The conclusion that DHE causes a disordering effect on the packing of the mixed interdigitated bilayers echoes the idea (Chong & Choate, 1989) that sterols may have a function in preventing lipids from forming highly ordered interdigitated structures in natural membranes. However, whether C(18):C(10)PC maintains an interdigitated structure in the presence of DHE and whether DHE interdigitates with C(18):C(10)PC remain to be explored.

Registry No. C(18):C(10)PC, 17511-04-5; DHE, 516-85-8.

REFERENCES

Archer, D. B. (1975) *Biochem. Biophys. Res. Commun. 66*, 195–201.

Bar, L., Chong, P. L.-G., Barenholz, Y., & Thompson, T. E. (1989) *Biochim. Biophys. Acta 983*, 109–112.

Bartlett, G. R. (1959) *J. Biol. Chem. 234*, 466–468.

Boggs, J. M., & Mason, J. T. (1986) *Biochim. Biophys. Acta 863*, 231–242.

Chong, P. L.-G., & Thompson, T. E. (1986) *Biochim. Biophys. Acta 863*, 53–62.

Chong, P. L.-G., & Choate, D. (1989) *Biophys. J. 55*, 551–556.

Chong, P. L.-G., Van der Meer, W. B., & Thompson, T. E. (1985) *Biochim. Biophys. Acta 813*, 253–265.

Chong, P. L.-G., Bar, L., Barenholz, Y., & Thompson, T. E. (1989) in *Fluorescent Biomolecules* (Jameson, D. M., & Reinhart, G. D., Eds.) p 374, Plenum Press, New York.

Cortijo, M., Alonso, A., Gómez-Fernandez, J. C., & Chapman, D. (1982) *J. Mol. Biol. 157*, 597–618.

Estep, T. N., Mountcastle, D. B., Biltonen, R. L., & Thompson, T. E. (1978) *Biochemistry 17*, 1984–1989.

Fischer, R. T., Stephenson, F. A., Shaffee, A., & Schroeder, F. (1985) *J. Biol. Phys. 13*, 13–14.

Gratton, E., & Limkeman, M. (1983) *Biophys. J. 44*, 315–324.

Hale, J. E., & Schroeder, F. (1982) *Eur. J. Biochem. 122*, 649–661.

Hinz, H. J., & Sturtevant, J. M. (1972) *J. Biol. Chem. 247*, 3697–3700.

Houslay, M. D., & Stanley, K. K. (1982) in *Dynamics of Biological Membranes* (Houslay, M. D., & Stanley, K. K., Eds.) pp 75–81, Wiley, New York.

Huang, C., & Mason, J. T. (1986) *Biochim. Biophys. Acta 864*, 423–470.

Huang, C., Lapiedes, J. R., & Levin, I. W. (1982) *J. Am. Chem. Soc. 104*, 5926–5930.

Huang, C., Mason, J. T., & Levin, I. W. (1983) *Biochim. Biophys. Acta 22*, 2775–2780.

Hui, S. W. (1988) in *Biology of Cholesterol* (Yeagle, P. L., Ed.) pp 213–231, CRC Press, Boca Raton, FL.

Hui, S. W., & Huang, C. (1986) *Biochemistry 25*, 1330–1335.

Hui, S. W., Mason, J. T., & Huang, C. (1984) *Biochemistry 23*, 5570–5577.

Jameson, D. M., & Gratton, E. (1983) in *New Directions in Molecular Luminescence* (Eastwood, D., Ed.) pp 67–81, American Society for Testing and Materials, Philadelphia, PA.

Kao, Y., & Chong, P. L.-G. (1989) *Biophys. J. 55*, 326a.

Ladbrooke, B. D., Williams, R. M., & Chapman, D. (1968) *Biochim. Biophys. Acta 150*, 333–340.

Lakowicz, J. R., Cherek, H., Maliwal, B. P., Gratton, E., & Limkeman, M. (1984) *Biophys. J. 46*, 463–477.

Lakowicz, J. R., Cherek, H., Maliwal, B. P., & Gratton, E. (1985) *Biochemistry 24*, 376–383.

Lentz, B. R., Freire, E., & Biltonen, R. L. (1978) *Biochemistry 17*, 4475–4480.

Levin, I. W., Thompson, T. E., Barenholz, Y., & Huang, C. (1985) *Biochemistry 24*, 6282–6286.

Mabrey, S., Mateo, P. L., & Sturtevant, J. M. (1978) *Biochemistry 17*, 2464–2468.

Mason, J. T. (1988) *Biochemistry 27*, 4421–4429.

Mason, J. T., Huang, C., & Biltonen, R. L. (1981) *Biochemistry 20*, 6086–6092.

Mattai, J., Sripada, P. K., & Shipley, G. G. (1987) *Biochemistry 26*, 3287–3297.

McIntosh, T. J., Simon, S. A., Ellington, J. C., Jr., & Porter, N. A. (1984) *Biochemistry 23*, 4038–4044.

Muczynski, K. A., & Stahl, W. L. (1983) *Biochemistry 22*, 6037–6048.

Nemecz, G., Fontaine, R. N., & Schroeder, F. (1988) *Biochim. Biophys. Acta 943*, 511–521.

Piston, D. W., Marriott, G., Radivoyevich, T., Clegg, R. M., Jovin, T. M., & Gratton, E. (1989) *Rev. Sci. Instrum.* (submitted for publication).

Rogers, J., Lee, A. G., & Wilton, D. C. (1979) *Biochim. Biophys. Acta 552*, 23–37.

Schroeder, F., Barenholz, Y., Gratton, E., & Thompson, T. E. (1987) *Biochemistry 26*, 2441–2448.

Singer, S. J., & Nicolson, G. I. (1972) *Science 175*, 720–731.

Slater, J. L., & Huang, C. (1988) *Prog. Lipid Res. 27*, 325–359.

Smutzer, G. (1988a) *Biochim. Biophys. Acta 958*, 323–333.

Smutzer, G. (1988b) *Biochim. Biophys. Acta 946*, 270–280.

Smutzer, G., & Yeagle, P. L. (1985) *Biochim. Biophys. Acta 814*, 274–280.

Smutzer, G., Crawford, B. F., & Yeagle, P. L. (1986) *Biochim. Biophys. Acta 862*, 361-371.
Weber, G. (1978) *Acta Phys. Pol., A A54*, 859-865.
Wong, P. T. T., & Huang, C. (1989) *Biochemistry 28*, 1259-1263.
Xu, H., & Huang, C. (1987) *Biochemistry 26*, 1036-1043.
Xu, H., Stephenson, F. A., & Huang, C. (1987) *Biochemistry 26*, 5448-5453.
Yeagle, P. L., Bensen, J., Greco, M., & Arena, C. (1982) *Biochemistry 21*, 1249-1254.
Zannoni, C., Arcioni, A., & Cavatorta, P. (1983) *Chem. Phys. Lipids 32*, 179-250.

The *CYP2A3* Gene Product Catalyzes Coumarin 7-Hydroxylation in Human Liver Microsomes†

Shigeru Yamano, Jun Tatsuno, and Frank J. Gonzalez*
Laboratory of Molecular Carcinogenesis, National Cancer Institute, National Institutes of Health, Bethesda, Maryland 20892
Received August 23, 1989; Revised Manuscript Received October 6, 1989

ABSTRACT: Three cDNAs, designated IIA3, IIA3v, and IIA4, coding for P450s in the *CYP2A* gene subfamily were isolated from a λgt11 library prepared from human hepatic mRNA. Only three nucleotide differences and a single amino acid difference, $Leu_{160} \rightarrow$ His, were found between IIA3 and IIA3v, indicating that they are probably allelic variants. IIA4 displayed 94% amino acid similarity with IIA3 and IIA3v. The three cDNAs were inserted into vaccinia virus, and recombinant viruses were used to infect human hepatoma Hep G2 cells. Only IIA3 was able to produce an enzyme that had a reduced CO-bound spectrum with a λ_{max} at 450 nm. This expressed enzyme was able to carry out coumarin 7-hydroxylation (turnover number of 15 min^{-1}) and ethoxycoumarin O-deethylation. cDNA-expressed IIA3v and IIA4 failed to incorporate heme and were enzymatically inactive. Analysis of IIA proteins in human liver microsomes, using antibody against rat IIA2, revealed two proteins of 49 and 50 kDa, the former of which appeared to correlate with human microsomal coumarin 7-hydroxylase activity. A more striking correlation was found between IIA mRNA and enzyme activity. The rat antibody was able to completely abolish coumarin 7-hydroxylase activity in 12 liver samples. In addition, kinetics of coumarin metabolism in two livers were monophasic over the substrate concentration tested. K_m values obtained from human liver (2.3 μM) were similar to those obtained from lysates of hepatoma cells expressing IIA3 (3.6-7.1 μM). These data establish that the *CYP2A3* gene product is primarily responsible for coumarin 7-hydroxylase activity in human liver. The level of expression of this activity varied up to 40-fold between livers. Levels of IIA mRNA also varied significantly between liver specimens, and three specimens had no detectable mRNA.

Cytochrome P450s[1] are the principal enzymes involved in the metabolism of foreign compounds including drugs, carcinogens, plant metabolites, and environmental contaminants. Nine P450 gene families exist in mammals (Nebert et al., 1989). The *CYP2* family is composed of eight subfamilies, some of which contain a number of P450s. The enzymes within these subfamilies catalyze the oxidation of numerous chemicals. Many of these enzymes are also species-specific. Species specificity can be illustrated by analyzing the metabolism of androgenic steroids. These reactions are not thought to be of physiological importance but may simply reflect the similarities in basic structures of steroids and plant-derived chemicals or stress metabolites, phytoalexins. P450s in rodents oxidize testosterone at numerous positions (Waxman, 1988) whereas human P450s produce primarily the 6β-hydroxytestosterone metabolite (Waxman et al., 1988). On the basis of these and other known species-specific metabolisms, it is becoming more important to characterize human P450s. Indeed, several P450 forms have been purified from human liver specimens (Distlerath & Guengerich, 1987). This direct approach is rather difficult for most laboratories due to the dearth of human liver specimens, the genetic heterogeneity between different livers, and the difficulty in purifying these enzymes, particularly those present at low levels.

Human P450s can also be characterized through cDNA cloning and expression. Antibodies and cDNA probes against rat P450s and P450 mRNAs, respectively, can be used to isolate the cDNAs from human liver libraries. Due to sequence similarities and multiplicity of P450s within gene subfamilies, a single rodent probe can identify multiple human cDNAs.

Previously, we used the rat IIA1 cDNA (Nagata et al., 1987) to isolate a cDNA from a human liver λgt11 library. The complete sequence of IIA3 was recently reported by us (Yamano et al., 1989b) and others (Miles et al., 1989). In the present report, the sequences of two additional variants of IIA3, one of which has an amino acid substitution, designated IIA3v, and a cDNA corresponding to a second gene

†S.Y. was supported by a Japanese Overseas Cancer Fellowship of the Foundation for Promotion of Cancer Research, and J.T. was supported by the Mitsubishi Kasei Corp., Yokohama, Japan.

[1] The nomenclature used in this report is that described by Nebert et al. (1989). The proteins and mRNAs are designated IIA3, IIA3v, and IIA4. The IIA3 cDNA, characterized in the present study, appears to be an allelic variant of that cDNA isolated in an earlier report (Yamano et al., 1989b). Since the deduced protein sequences of these two cDNAs are identical, we chose not to designate them with different names in the present report. The IIA3v cDNA displays only three nucleotide differences and one amino acid difference with the IIA3 cDNA characterized in this study; therefore, these cDNAs also are probably allelic variants. However, since IIA3v contains an amino acid difference ($Leu_{160} \rightarrow$ His) and could not be expressed into active P450, we chose to call it a variant (IIA3v variant). The genes encoding IIA3/IIA3v and IIA4 mRNAs are designated *CYP2A3* and *CYP2A4*, respectively.